

# Theoretical investigation of vanadium oxide film with surface microstructure

WEI HONG\*, ZHE WANG, QIAN CHEN, CHUANXIANG SHENG, GUOHUA GU, PENG PENG LUO, YANG XIE

School of Electronic and Optical Engineering, Nanjing University of Science and Technology, Nanjing, China, 210094

\*Corresponding author: hongwei@njjust.edu.cn

This paper presents a method to design a surface microstructure of vanadium oxide to enhance optical absorption. This method, using a density of eigenfrequency, can be calculated by a planar wave expand method, to indicate the absorption efficiency of a dispersion material, which can be used as an approach method for further design. Based on this, a nanostructure-based vanadium oxide film is designed and simulated to validate this method. The simulation results show that the tendency of density of eigenfrequency is corresponding to the tendency of optical absorption enhancement. Moreover, this structure can achieve high optical broadband absorption when the material dispersion is considered. High optical absorption enhancement can be achieved by adjusting the geometrical parameters; our maximum overall enhancement absorption ratio was 31.84% at the metal phase, which can be attributed to the enhancement effect of a photonic band edge.

Keywords: vanadium oxide (VO<sub>2</sub>) film, surface microstructure, photonic band edge, dispersion material.

## 1. Introduction

Vanadium dioxide (VO<sub>2</sub>) is a metal–insulator transition (MIT) material which undergoes a structural transition from an insulating phase to a metallic phase at 68°C [1]. A reversible phase change occurs on a sub-picosecond time scale [1, 2]. By virtue of these characteristics, the material can be used in detectors, imaging devices, sensors, switches, and other applications [3–7]. MANNING *et al.*, for example, proposed VO<sub>2</sub> as a thermal material for smart windows [4]. YANFENG GAO *et al.* has also conducted extensive research on this subject [5]. The low transparency and insufficient phase-transition efficiency limit the application of VO<sub>2</sub>, however, especially in regards to short-wave imaging systems or infrared (IR) detectors.

Electromagnetic absorption enhancement based on structured surfaces has received a great deal of research attention in recent years [8–10]. Controlling and manipulating the spectral absorption properties of materials in the IR range are an area of particularly active research; successful techniques could enable advances in applications such as target recognition and IR imaging sensors [10]. KOCER *et al.* presented an infrared res-

onant absorber based on hybrid gold-VO<sub>2</sub> nanostructures that can reach up to 96% absorption [11]. Such demonstrated a metal-VO<sub>2</sub> film to enhance optical transmission through subwavelength hole-arrays via temperature-controlled modulation, where the transmitted intensity ratio increases by a factor of 8 as the VO<sub>2</sub> goes from the semiconductor to the metal phase [12].

Recently, the use of surface microstructures for the enhancement of photon trapping efficiency has been investigated at length [13–16] and many applications have been proposed to improve the absorption efficiency of solar cells [17, 18]. Because large in-plane optical resonance can appear at the photonic band edge (PBE), incident light from the free space is coupled into the photonic band edge mode and longer interaction time with the material is achieved; these factors enhance the optical absorption. Although many researchers have discussed the band structure, or absorption spectrum, with dispersion materials, they mostly have used the finite-difference time-domain (FDTD) method [14].

In this paper, we focus on a fast and convenient method to indicate the optical absorption enhancement of a microstructure surface based VO<sub>2</sub>. Since the slow Bloch mode [16] exists in this structure, the incident light can couple into the microstructure surface by resonance at the band edge. It is then trapped by the microstructure surface to ultimately enhance absorption. We can consider the density of eigenfrequency (DoE), existing at the photonic band edge ( $\Gamma$  point), to indicate the absorption efficiency of a dispersion material. Moreover, the DoE at  $\Gamma$  point can be calculated by a planar wave expand method, which is fast and convenient. This method is useful to design a periodical structure as a preliminary proceeding for careful design with FDTD method or other full wave simulation methods. Based on this, a nanostructure-based vanadium oxide film is designed and simulated by FDTD method to validate our method. The method proposed here can be used in other VO<sub>2</sub> applications to enhance the absorption efficiency, such as high efficiency mid-IR to NIR conversion.

## 2. Theoretical investigation of PBE for dispersion material

The complex refractive index ( $n + ik$ ) used in our model, as shown in Fig. 1, sits on the VO<sub>2</sub> thin film in the wavelength range of 700 to 1700 nm. Considering the insulator-to-metal (IM) transition of VO<sub>2</sub>, the index is given both in the insulator phase and in metal phase. There is an obvious difference between these two states. The absorption coefficient  $k$  is larger in the metal phase than in the insulator phase, indicating a larger infrared absorption at the metal phase.

To enhance the film absorption, a microstructure layer is designed to confine light. A schematic diagram of the proposed structure, considering a microstructure film, is depicted in Fig. 2. As shown in Fig. 2, the input light is incident from the  $z$  direction and the surface microstructure film is placed at the  $xy$  plane. A layer of square-arrayed VO<sub>2</sub> rods formed by a square lattice and cylinder as a unit cell is sculptured on the surface of the VO<sub>2</sub> layer. The unit cell period is labeled as  $a$  and the VO<sub>2</sub> rod radius is labeled as  $r$ .

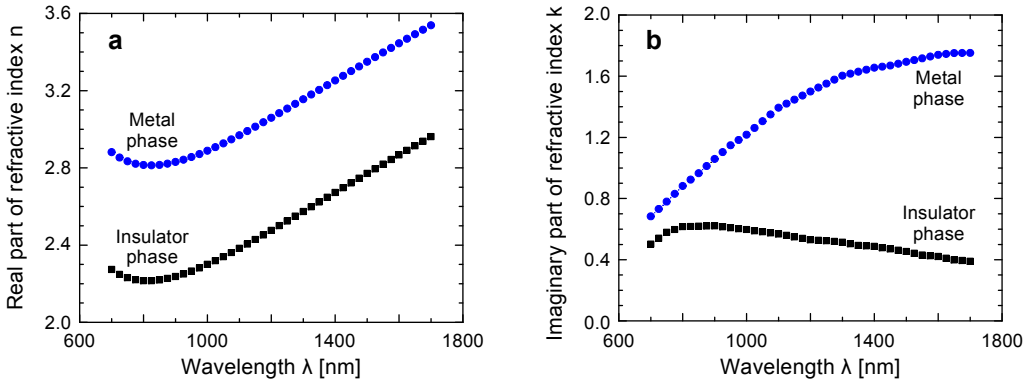


Fig. 1. The real (a) and imaginary (b) part of complex refractive index of VO<sub>2</sub> for insulator and metal phases.

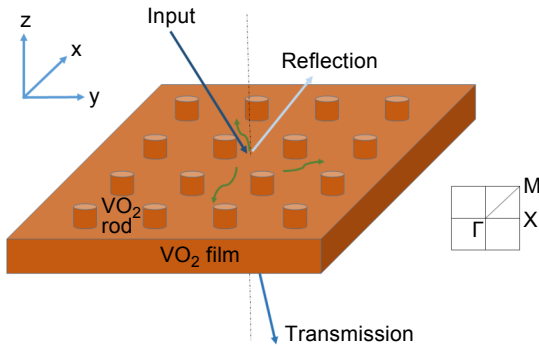


Fig. 2. Schematic diagram of VO<sub>2</sub> film surface microstructure.

The band structure of the square-lattice VO<sub>2</sub> rod, the insulator phase, is shown in Fig. 3, using planar wave expand (PWE) method, where  $r/a$  is set to 0.4. The vertical axis represents the normalized frequency by the unit of  $a/\lambda$ , where  $\lambda$  represents the wavelength. The horizontal axis shows the high symmetry wave vector points ( $M, \Gamma, K$ ) of the irreducible Brillouin zone (IBZ). At those points, the so-called band edge, waves

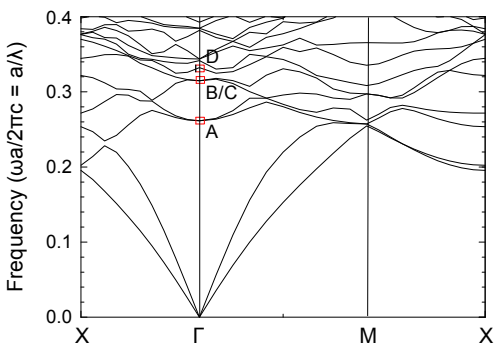


Fig. 3. Band structure of the 2D square VO<sub>2</sub> rod microstructure in Fig. 2.

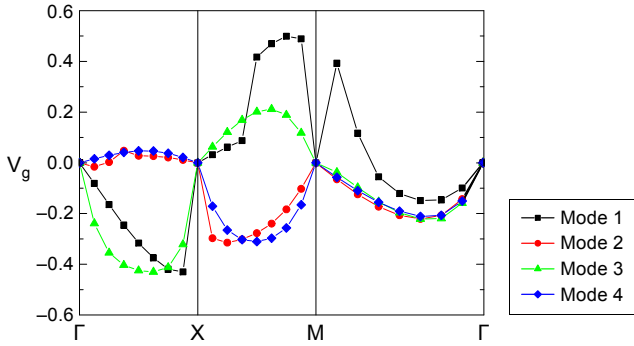


Fig. 4. Group velocity of the four lowest eigenmode.

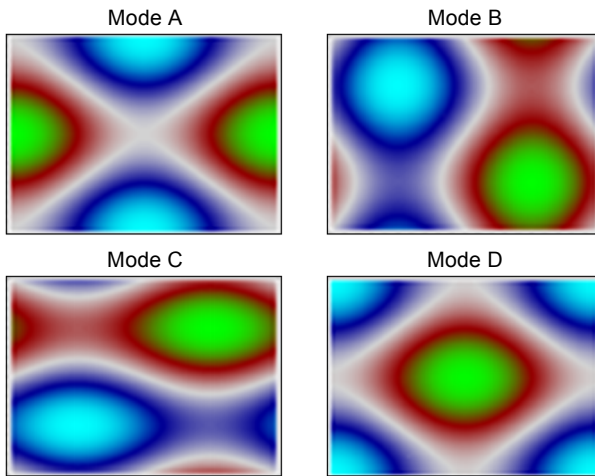


Fig. 5. PBE modes for the lowest three frequencies.

propagating in different directions are coupled and a standing wave is formed [14]. The band edge at  $\Gamma$  is even more interesting, as it gives the in-plane coupling of light which can exist in Bloch mode. The group velocities of the four lowest eigenfrequencies are plotted in Fig. 4, where the group velocities at  $\Gamma$  points are all zero indicating that the incident frequency at  $\Gamma$  points should be a standing wave in the microstructure. Four PBE modes with the lowest three frequencies, marked by a square in Fig. 3, are plotted in Fig. 5. PBE modes B and C have a standing wave field distribution with degenerate orthogonal modes, and PBE modes A and D have standing waves with rotational electric fields. The standing wave indicates that incident light can be trapped perfectly around these frequency points.

The refractive index of a dispersion material is altered with frequency and can be exploited to achieve a wide band PBE mode absorber. It is difficult to calculate the band structure of a dispersion material using PWE method. Considering the material dispersion of  $\text{VO}_2$ , we calculated the eigenfrequencies at  $\Gamma$  points with PWE for each

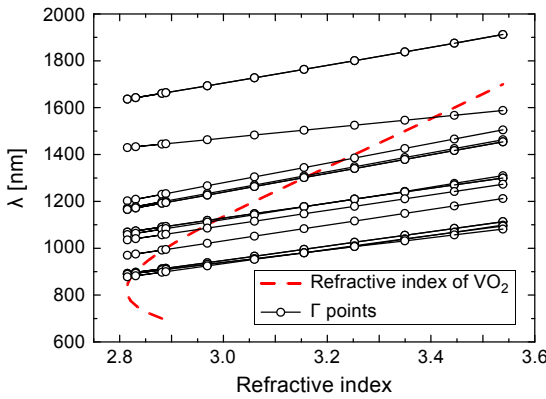


Fig. 6. The eigenfrequencies at  $\Gamma$  point for a dispersion material ( $\text{VO}_2$ ).

material index (insulator phase of  $\text{VO}_2$ ), as marked with solid lines in Fig. 6. The refractive index of  $\text{VO}_2$  is marked with a dashed line in Fig. 6 and the eigenfrequencies at  $\Gamma$  point for a dispersion material can be found at the cross points. There are numerous eigenfrequencies at  $\Gamma$  point in the range from 800 to 1600 nm, implying that absorption enhancement is strengthened in a wide frequency range.

The cross points of the eigenfrequencies (solid lines) and dispersion line (dashed line) are: 1562.72 nm (1), 1385.43 nm (1), 1297.83 nm (2), 1124.96 nm (3), 1086.28 nm (2), 991.47 nm (2), 895.69 nm (1), and 881.31 nm (3); numbers in parentheses indicate the number of eigenfrequency, which is defined as the number of cross points.

To determine the relation of the numbers of eigenfrequency at  $\Gamma$  point and the enhancement of absorption, we define a new parameter as the DoE, denoted as  $\rho$ , in the following equation:

$$\rho(\lambda) = \frac{N}{\lambda_{n+1} - \lambda_{n-1}} \quad (1)$$

where  $N$  is the number of eigenfrequency at the cross points,  $\lambda_n$  is the wavelength at the same eigenfrequency, and  $\lambda_{n+1}$  and  $\lambda_{n-1}$  are the neighbor wavelengths of  $\lambda_n$ .

### 3. Results and discussion

#### 3.1. Absorption enhancement of a microstructure film

The complex refractive index of  $\text{VO}_2$  film is used here to calculate absorption characteristics with the FDTD method, run in commercial software Lumerical. The optical absorptivity is calculated by  $1 - |T| - |R|$ , where  $T$  is the transmittivity and  $R$  is the reflectivity. The thickness of the  $\text{VO}_2$  film is fixed at 400 nm, the height of the  $\text{VO}_2$  rod is set to 200 nm, and the lattice period  $a$  is set to 500 nm. Figure 7 shows a comparison of the absorption ratio vs. the wavelength of a  $\text{VO}_2$  thin film with or without microstructure patterns. The microstructure  $\text{VO}_2$  film has higher absorption at insulator and

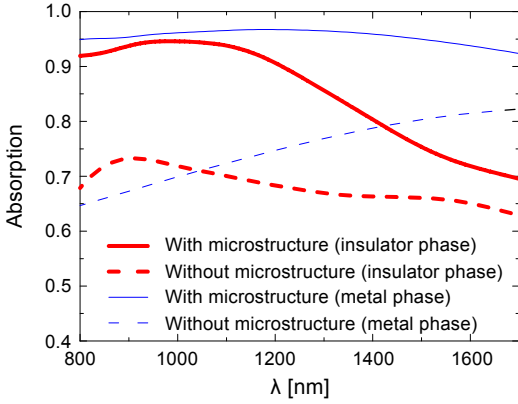


Fig. 7. Absorption efficiency as function of wavelength for the VO<sub>2</sub> film with or without microstructure, both insulator phase and metal phase are considered.

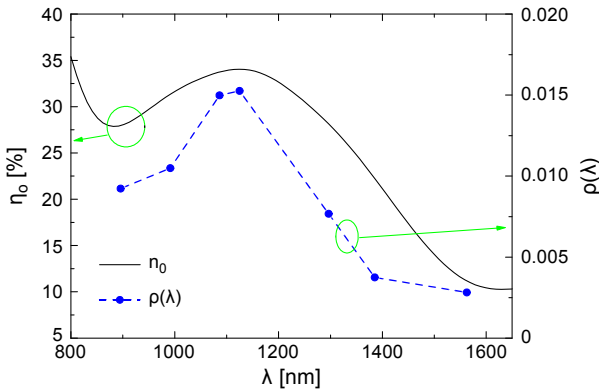


Fig. 8. Enhancement ratio at insulator phase with surface microstructure (solid line, left axis) and DoE (dashed line, right axis).

metal phase states in the NIR frequency range. The highest absorption ratio we observed is 1100 nm for the insulator phase, as indicated by the DoE we calculated, which is shown in Fig. 8.

The enhancement absorption ratio parameter  $\eta$  is defined to evaluate the impact of structure parameters on the absorption

$$\eta = \frac{\int \lambda A_{pc}(\lambda) d\lambda - \int \lambda A_{film}(\lambda) d\lambda}{\int \lambda A_{film}(\lambda) d\lambda} \tag{2}$$

where  $A_{pc}(\lambda)$  is the absorptivity for the film with surface pattern and  $A_{film}(\lambda)$  is the absorptivity for the same film without surface pattern.

### 3.2. Optimization of microstructure parameters

The microstructure is sensitive to the structure parameters and material index, so the microstructure layer should be optimized in order to secure a high absorption. Here, we focus our effort in searching for the best possible structure parameter to optimize the results.

To make sure that the enhanced absorption region is in the NIR range, we fixed  $a$  to 500 nm. This way,  $r$  affects the band structure and changes the absorption ratio  $A(\lambda)$ . The overall enhancement ratio  $\eta_o$  which shows the average enhancement absorption in the frequency range between 700 and 1700 nm, can be calculated with Eq. (2).

The  $r$  is swept to find the highest  $\eta_o$ . Here, the  $r$  is scanned from 25 to 225 nm by a step of 25 nm; the  $\eta_o$  varies with  $r/a$  as plotted in Fig. 9a. When  $r/a < 0.175$ , the  $\eta_o$  is negative. This means that the frequency range of our interest is in the stop band and the surface pattern reduces the absorption ratio. With careful design, the working condition should be  $r/a \geq 0.2$ . The maximum enhancement ratio (28.47% for the insulator phase) can be obtained when  $r/a = 0.35$  for both the insulator and metal phases.

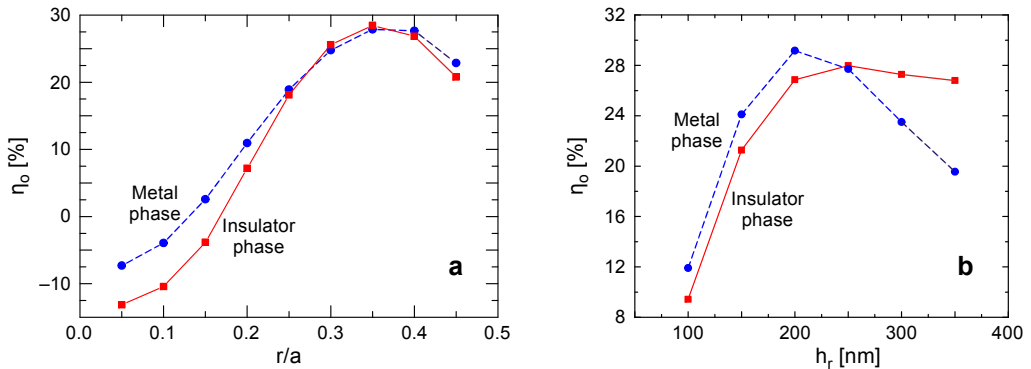


Fig. 9. Overall enhancement absorption ratio with structure parameter of microstructure pattern with  $r/a$  (a) and with  $h_r$  (b). Insulator-to-metal (IM) transition is also considered.

Next, we consider the thickness of the microstructure  $h_r$ . The  $h_r$  value changes from 100 to 350 nm by a step of 50 nm in our simulation (Fig. 9b). The impact of  $h_r$  is different from that of  $r$ : the maximum  $\eta_o$  diverges to different  $h_r$  values for the insulator phase,  $h_r = 300$  nm with  $\eta_o = 27.97\%$ , and metal phase,  $h_r = 200$  nm with  $\eta_o = 31.84\%$ .

## 4. Conclusions

In this study, we investigated a method to indicate the optical absorption enhancement of a microstructure surface based  $\text{VO}_2$ . The DoE parameter, as an approximation method, is proposed to indicate the absorption efficiency of dispersion materials and the DoE at  $\Gamma$  point can be calculated by the planar wave expand method, which is fast and convenient. Based on this, we achieved a considerable absorption enhancement (maximum

ratio of 31.84%) due to effects of the surface microstructure, and the enhancement spectrum is well agreed with the tendency of DoE. Following this, the structure parameter, lattice rod radius, and microstructure pattern thickness were all optimized to achieve these results. In the future, we plan to examine other microstructure patterns and further improve other transport properties of the film microstructure. We hope that this work will extend the use of VO<sub>2</sub> films in IR detectors and other applications.

*Acknowledgements* – This work was supported by the Natural Science Foundation of Jiangsu Province, China, under Grant No. BK20140799.

## References

- [1] MORIN F.J., *Oxides which show a metal-to-insulator transition at the Neel temperature*, Physical Review Letters **3**(1), 1959, pp. 34–36.
- [2] CAVALLERI A., TÓTH Cs., SIDERS C.W., SQUIER J.A., RÁKSI F., FORGET P., KIEFFER J.C., *Femtosecond structural dynamics in VO<sub>2</sub> during an ultrafast solid-solid phase transition*, Physical Review Letters **87**(23), 2001, article ID 237401.
- [3] LYSENKO S., RÚA A., VIKHNIN V., FERNÁNDEZ F., LIU H., *Insulator-to-metal phase transition and recovery processes in VO<sub>2</sub> thin films after femtosecond laser excitation*, Physical Review B **76**(3), 2007, article ID 035104.
- [4] MANNING T.D., PARKIN I.P., CLARK R.J.H., SHEEL D., PEMBLE M.E., VERNADOU D., *Intelligent window coatings: atmospheric pressure chemical vapour deposition of vanadium oxides*, Journal of Materials Chemistry **12**(10), 2002, pp. 2936–2939.
- [5] YANFENG GAO, HONGJIE LUO, ZONGTAO ZHANG, LITAO KANG, ZHANG CHEN, JING DU, MINORU KANEHIRA, CHUANXIANG CAO, *Nanoceramic VO<sub>2</sub> thermochromic smart glass: a review on progress in solution processing*, Nano Energy **1**(2), 2012, pp. 221–246.
- [6] BONORA S., BORTOLOZZO U., RESIDORI S., BALU R., ASHRIT P.V., *Mid-IR to near-IR image conversion by thermally induced optical switching in vanadium dioxide*, Optics Letters **35**(2), 2010, pp. 103–105.
- [7] SAJEEV JOHN, *Strong localization of photons in certain disordered dielectric superlattices*, Physical Review Letters **58**(23), 1987, p. 2486.
- [8] YABLONOVITCH E., *Inhibited spontaneous emission in solid-state physics and electronics*, Physical Review Letters **58**(20), 1987, p. 2059.
- [9] IMADA M., NODA S., CHUTINAN A., TOKUDA T., MURATA M., SASAKI G., *Coherent two-dimensional lasing action in surface-emitting laser with triangular-lattice photonic crystal structure*, Applied Physics Letters **75**(3), 1999, pp. 316–318.
- [10] TAESUNG KIM, LEISHER P.O., DANNER A.J., WIRTH R., STREUBEL K., CHOQUETTE K.D., *Photonic crystal structure effect on the enhancement in the external quantum efficiency of a red LED*, IEEE Photonics Technology Letters **18**(17), 2006, pp. 1876–1878.
- [11] KOCER H., BUTUN S., BANAR B., WANG K., TONGAY S., JUNQIAO WU, AYDIN K., *Thermal tuning of infrared resonant absorbers based on hybrid gold-VO<sub>2</sub> nanostructures*, Applied Physics Letters **106**(16), 2015, article ID 161104.
- [12] SUH J.Y., DONEV E.U., LOPEZ R., FELDMAN L.C., HAGLUND R.F. JR., *Modulated optical transmission of subwavelength hole arrays in metal-VO<sub>2</sub> films*, Applied Physics Letters **88**(13), 2006, article ID 133115.
- [13] DUCHÉ D., ESCOUBAS L., SIMON J.-J., TORCHIO P., VERVISCH W., FLORY F., *Slow Bloch modes for enhancing the absorption of light in thin films for photovoltaic cells*, Applied Physics Letters **92**(19), 2008, article ID 193310.
- [14] YUNLU XU, TAO GONG, MUNDAY J.N., *The generalized Shockley–Queisser limit for nanostructured solar cells*, Scientific Reports **5**, 2015, article ID 13536.



- [15] ZHE WANG, WEI HONG, QIAN CHEN, GUOHUA GU, JUN LU, *Enhanced optical absorption in VO<sub>2</sub> film using photonic crystal*, 11th Conference on Lasers and Electro-Optics Pacific Rim (CLEO-PR), August 24–28, 2015, Busan, South Korea, article ID 27P\_15.
- [16] NODA S., YOKOYAMA M., IMADA M., CHUTINAN A., MOCHIZUKI M., *Polarization mode control of two-dimensional photonic crystal laser by unit cell structure design*, *Science* **293**(5532), 2001, pp. 1123–1125.
- [17] RUFANGURA P., SABAH C., *Design and characterization of a dual-band perfect metamaterial absorber for solar cell applications*, *Journal of Alloys and Compounds* **671**, 2016, pp. 43–50.
- [18] RUFANGURA P., SABAH C., *Dual-band perfect metamaterial absorber for solar cell applications*, *Vacuum* **120**, 2015, pp. 68–74.

*Received March 11, 2017  
in revised form April 13, 2017*